31st Congress of the International Council of the Aeronautical Sciences

Belo Horizonte, Brazil; September 09-14, 2018

DETECTING HIGH-ALTITUDE ICE CRYSTAL (HAIC) ICING EVENTS FROM TOTAL AIR TEMPERATURE (TAT) ANOMALIES

Álvaro Rodríguez-Sanz*, Rosa María Arnaldo*, Eduardo Sánchez Ayra*, **, Fernando Gómez Comendador*

***Universidad Politécnica de Madrid (UPM), **IBERIA Airlines**

Keywords: *HAIC, TAT anomalies, failure heuristic, system reliability, FDM*

Abstract

High-Altitude Ice Crystals (HAIC) constitute a hazard to commercial aircraft flying near deep convective weather due to jet-engine power loss and air data probes malfunction. HAIC can stick to warm metal surfaces in jet-engines and cause engine surge, stall, flameout and rollback, power loss, as well as engine compressor damage due to ice shedding. Along with these events, disruption to aircraft systems are noted when HAIC are ingested into air data probes (Pitot tube and/or Total Air Temperature -TAT- sensor), causing erroneous measurements of temperature and air speed. Particularly, the TAT probe incorrectly reporting zero degrees Celsius or in error is known to be evidence of ice crystals in the atmosphere surrounding the aircraft. TAT anomalies are due to the accumulation of ice crystals in the TAT sensor, producing a zero degrees Celsius reading, generating failures in airspeed indicators and acting as potential incident/accident precursors.

In this paper, TAT events are analyzed from pilot reports and from Flight Data Monitoring (FDM). TAT FDM data analysis covers two families of engines: i) CFM56/20 (twin-engine configuration) on A319, A320 and A321 fleets (medium range), and A330 fleet (long range); ii) Rolls-Royce Trent 500 (four-engine configuration) on A340 fleet (long range).

Based on these analyses, this paper presents a sensor failure tolerant heuristic that generates a reliability indicator, founded on the differences between the TAT and the engine's inlet temperature sensors. It aims to provide early warnings to pilots regarding HAIC events and prevent potential data errors and system failures.

1 Introduction

High-Altitude Ice Crystals (HAIC) constitute a hazard to commercial aircraft flying near deep convective weather due to jet engine power loss and air data probes malfunction [1]. In the mid-90s, several commercial jet airplanes experienced frequent engines power-loss in ice particle conditions, which fostered research and awareness, resulting in the identification of similar events on other aircraft. Since the mid-90s, reported events have increased and have sparked interest within the industry [2]. Therefore, the frequency of power-losses and other engine damages in commercial airplane jet engines flying under ice particle conditions has become a widespread safety concern during the last decades [3]. Significant research efforts have been devoted to understanding this phenomenon and mitigating its related risks. Despite the focus on the possible engine damages derived from HAIC, no significant aviation accidents have occurred due to this cause. Nevertheless, the last decade has registered two accidents caused by non-detected erroneous information sent to the autopilot due to high concentrations of ice crystals obstructing pitot probes: i) the accident of the Air France AF447 from Rio de Janeiro to Paris on 1 January 2009 [4], and ii) the accident of the Swiftair AH5017 on 24 July 2014 in the region of Gossi, in Mali [5]. It is necessary to develop methodologies that help identify erroneous measurements due to ice crystals events. However, detecting HAIC conditions is a difficult task, as there are not proper ice particle detection technologies or devices that can be used on board of commercial aircraft.

Small particles, such as ice crystals in high concentrations near thunderstorms, are invisible to on-board weather radar, even though they may comprise most of the total mass of a cloud. Ice crystals can stick to warm metal surfaces of a jet's engines, and when enough ice accumulates and sheds into the engine it can cause engine surge, stall, flameout and rollback, power loss, as well as engine compressor damage due to ice shedding [6,7]. Along with these events, disruption to the air aircraft data system are noted when ice crystals are ingested into various inlets, causing erroneous measurements of temperature, air speed, and angle of attack [2]. Particularly, the airplane total air temperature (TAT) probe erroneously reporting zero degrees Celsius or in error, is known to be evidence of ice crystals in the atmosphere. TAT anomalies are due to the partial fusion of the accumulation of ice crystals around the thermocouple, producing a zero degrees Celsius reading [8].

This paper follows latest scientific studies and statistical analyses, which relate total air temperature (TAT) anomalies data to ice crystal exposure [2], to propose a potential on-board system that provides early warning to pilots flying in HAIC conditions. This system aims to mitigate HAIC risk and prevent accidents like the ones mentioned above. The detection methodology is based on a heuristic that generates a reliable HAIC alert, based on detected Total Air Temperature (TAT) anomalies, i.e. TAT erroneously reporting zero degrees Celsius. The heuristic is tolerant to failures of the temperature sensors and is based on the measurements of the differences between the TAT and the engine's inlet temperature sensors. This heuristic is supported by the FDM (Flight Data Monitoring) analysis of more than 285,000 flights covering a period of almost 4 years, to robustly identify and detect anomalies in TAT. This TAT FDM data analysis has included two families of engines: i) CFM56/20 (twin-engine configuration) on A319, A320 and A321 fleets (medium range), and A330 fleet (long range); ii) Rolls-Royce Trent 500 (four-engine configuration) on A340 fleet (long range). The study is completed with an exploratory data analysis of TAT anomalies and a probabilistic model to predict and evaluate potential events for the appraised routes.

2 HAIC - High Altitude Ice Crystals

Deep convective clouds above the freezing level contain high concentrations of small ice crystals: up to 8 g/m^3 with particles from microns up to millimeter size [9]. These particles are called High Altitude Ice Crystals (HAIC). Ice particles can enter the engine and bounce off surfaces colder than freezing (inlet, fan and spinner). Once these particles reach surfaces warmer than freezing in the engine core, some of the small particles can melt and create a film of water on the surface to which additional incoming ice crystals can stick. This process gradually reduces the temperature of the surface until ice can begin to build up. Consequently, HAIC can cause engine instability, power loss or damage; and air data sensor obstruction [10,11].

A triple strategy is currently being implemented to safely fly through High Ice Water Content (HIWC) regions: engine design regulations, improved weather forecasting tools and on-board detection [2]. This paper focuses on the last one.

Identifying HAIC conditions is a difficult task. On-board weather radar can detect large particles such as hail, rain, and large ice crystal masses (snowflakes). However, small particles, such as ice crystals in high concentrations near thunderstorms, are invisible to on-board weather radar, even though they may comprise most of the total mass of a cloud [1]. Sophisticated satellite radar technology has been used to detect crystals smaller than the lower limit of on-board weather radar [12]. Nevertheless, there is still a lack of a direct indicator for HAIC encounters.

3 Total Air Temperature (TAT) anomalies as indicator of HAIC

Unusual conditions that are typically found during engine ice crystal power-loss events can be used to identify possible situations of ice crystal risk (e.g. high altitude convective clouds, no significant airframe icing, "heavy rain" on the windscreen, light and moderate turbulence).

Particularly, total air temperature (TAT) anomalies (reading zero, or in error) have been reported to occur during some engine power loss events due to HAIC events. Moreover, the airplane total air temperature (TAT) probe erroneously reporting zero degrees Celsius is known to be evidence of ice crystals in the atmosphere [2].

This anomaly is due to ice crystals building up in the area where the thermocouple is located, where the particles are partly melted by the heater causing the zero degrees Celsius reading [1,10]. In some cases, TAT anomalies ("flat-lined" at zero during a descent) may provide an early warning noticeable to pilots. In other cases, the error is too subtle to be directly detected by pilots, and TAT may not be a reliable indicator to provide early warning to pilots of high concentrations of ice crystals [2].

In this paper, we develop a methodology to identify potential HAIC events based on TAT anomalies. Particularly, this study aims to develop heuristics for FDM (Flight Data Monitoring) TAT events detection and to exploit flight data to gain insight on the frequency of occurrence, location, and magnitude of HAIC.

4 Development of a reliable TAT event indicator and Flight Data Monitoring (FDM) heuristic

In this work, a heuristic is developed to identify TAT events from the FDM (flight Data Monitoring) data analysis. This heuristic is tolerant to failures in temperature sensors and generates a reliable TAT event indictor based on the differences between the TAT and the engine's inlet temperature sensors. This heuristic has been used for an off-line analysis of TAT events but could also be implemented on board to provide early warning to pilots of high concentrations of ice crystals.

4.1 Engines analyzed

The developed TAT FDM data analysis covers two families of engines: i) CFM56/20 and ii) Rolls Royce Trent 500.

The CFM 56 family of turbofan engines is produced by CFMI (Commercial Fan Motor International). This type of engines integrates a control system called FADEC (Full Authority Digital Electronic Control) which provides full control of the aircraft to achieve a steady state and transient actions when operating in combination with aircraft subsystems. This system is based on a dual channel control unit: ECU (Electronic Control Unit).

These engines are used on the aircraft families of Airbus A319, A320 and A321, corresponding to short/medium haul aircraft in a twin-engine configuration, and on the Airbus A330 which is a long-haul aircraft with a twin-engine configuration.

Figure 1 illustrates the distribution of the sensors that allow monitoring the values of the pressure (P), temperature (T) and engine thrust (N) at the different stages of the air flow through the engine: P0, T49.5 (EGT), T25, N1, N2, T12, PS12, PS3, T3, T-CASE.

Figure 1. CFM 56 sensors

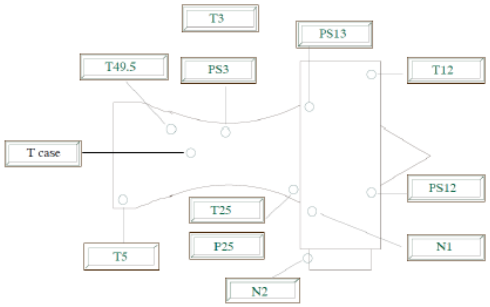

Since our study covers the loss of thrust and the failure of sensors exposed to high concentration of ice crystals, the indications of the following sensors are used to detect anomalies:

- T12: It is an electric sensor that measures the temperature, in Celsius degrees, of the air entering the engine before the airflow reaches the rotor (N1).
- PS12: It is an electric sensor that measures the pressure before the air flow enters the rotor (N1). Pressure is measured in PSI (pounds-force per square inch, lbf/in^2).
- N1: Rotation of the blades of the first stage of the low-pressure compressor, measured in % RPM.

- T49.5 (EGT - Exhaust Gas Temperature): It is the exhaust gas temperature, which is measured in Celsius degrees at the penultimate turbine stage.

Rolls Royce produces the RR Trend 500 family of turbofan engines. This engine is used on the Airbus A340-600, long haul aircraft equipped with four RR Trent 500 engines.

The RR Trent 500 integrates an interface called EIVMU (Engine Interface and Vibration Monitoring Unit), which is used to monitor the motor, and is associated with its own control unit: EEC (Electronic Engine Controller).

Figure 2 shows how the sensors that monitor the values of the pressure (P), temperature (T) and engine thrust (N) at the different stages of the airflow through the engine are distributed: P20, T20, N1, N2, N3, P0, P160, P25, P30, T30, EGT and P50.

As can be observed, the location and name of the sensors is very similar in both engines. For the RR Trent 500, the following sensors will be used to detect anomalies: T20, P20, N1 and EGT.

The T20 and P20 sensors measure the temperature and pressure of the air entering the engine.

Figure 2. Rolls Royce Trent 500 sensors

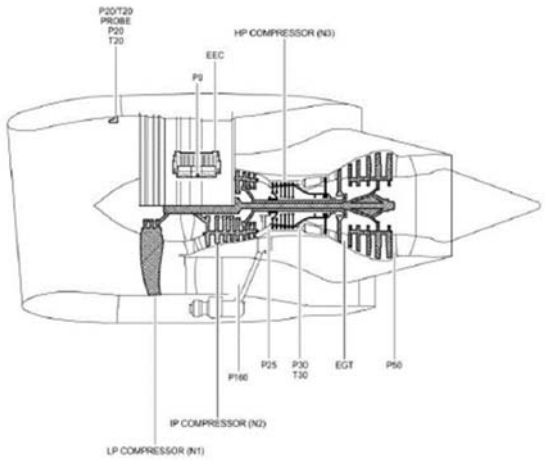

4.2 Initial heuristic to detect TAT anomalies

At cruising flight levels (above 20,000 ft), the air temperature is much lower than 0ºC, so readings close to 0ºC are detected as a measurement error in the sensor. This change in temperature is immediate and is associated with a possible event of ice crystals, which in some concentration can obstruct the TAT sensor, causing erroneous readings [2].

Therefore, a "TAT event" is initially identified when, at cruising levels, the TAT sensor produces a drastic change in its reading to levels between -3ºC and 3ºC. If this situation is detected during the FDR (Flight Data Recorder) analysis a TAT event report is produced.

The flowchart in Figure 3 summarizes the initial heuristic ("TAT event": at cruising levels the TAT sensor readings between -3°C and 3°C).

Figure 3. Flowchart for initial TAT event detection

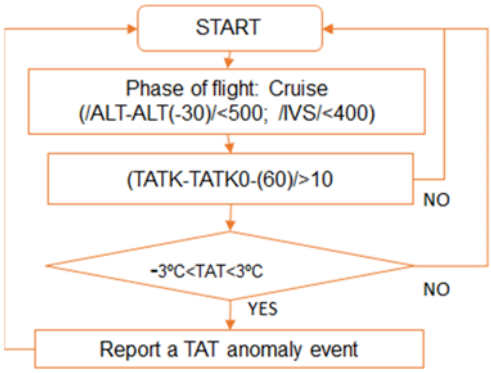

The heuristic monitors flight parameters every second (1Hz), although it can be programmed to operate at a different sampling frequency. As can be observed, the first step in the algorithm is to determine that the aircraft is in the cruise phase of flight. To do this, the algorithm verifies that the vertical speed (VS) is between -400 and 400 ft/min for 15 seconds and that the altitude is higher than 10,000 ft (these conditions discard climb and descend phases). Once detected that the aircraft is in the cruise phase, the next step is to avoid variations of the TAT due to changes in altitude, by limiting the altitude values so that in less than 30 seconds the aircraft has not ascended or descended more than 500 ft. The following step is to verify the rate of change of the TAT. TAT increases or decreases higher than 10ºC in 60 seconds are characterized as a possible case of TAT anomaly. Finally, it is verified that this increase in the slope of variation of the TAT, at some time of the following 5 minutes after the increase, reaches values ranging between -3º and 3º. The main limitation of this initial heuristic for detection of TAT anomalies is that it is restricted to the cruise phase.

4.2 Improved heuristic to detect TAT anomalies

The analysis of the FDR data and pilot reports of all the flights affected by a TAT anomaly, has enabled us to detect that there is a great correlation (R^2>0.9) between the measurements of the sensors at the engine's air inlet (T12 for CFM56 and T20 for Rolls Royce) and the TAT. Both sensors register virtually identical values of temperature, except when a TAT anomaly takes place. This phenomenon is illustrated on Figure 4.

Figure 4. TAT event

This feature allows us to improve the TAT detection heuristic and extend it to all flight phases. The new heuristic will be based on the differences between the TAT sensor and the sensors at the engine inlet (T12 for CFM56 and T20 for Rolls Royce)

The FDR analysis also showed that in certain situations, the T20 sensor of some of the Rolls Royce engine failed and took incorrect measurements. As the improved algorithm will incorporate information from T20 sensors, it must be resistant to T20 sensor failures. To increase the reliability of the detection algorithm, a check is incorporated to verify that the four sensors, in the case of four-engine aircraft, are in the same range.

The algorithm compares one by one the sensors in groups of three, as follows:

- Set A: Sensor 1 is compared with sensor 2 and with sensor 3. If they differ by more than 2ºC, Set A will be activated, otherwise it will remain deactivated.
- Set B: Sensor 1 is compared with sensor 3 and with sensor 4. If they differ by more than 2ºC, Set B will be activated, otherwise it will remain deactivated.
- Set C: Sensor 1 is compared with sensor 2 and with sensor 4. If one of them differs by more than 2°C, Set C will be activated, otherwise it will remain deactivated.

Then, depending on which set of sensors is activated, it will be possible to determine the sensor that generates erroneous measurements:

- Failure in engine T12 / T20 sensor 1: Occurs when all sets are activated.
- Failure in engine T12 / T20 sensor 2: Occurs when sets A and C are activated and B is deactivated.
- Failure in engine T12 / T20 sensor 3: Occurs when sets A and B are activated and C is deactivated.
- Failure in engine T12 / T20 sensor 4: Occurs when sets B and C are activated and A is deactivated.

If all sets are deactivated, it is concluded that data is within normal limits, and therefore, although there may be temperature variations, they will be neglected.

Once the measurements of the T12 / T20 sensors have been determined, data will be averaged and compared with the TAT. If in the previous process there was a fault in one sensor, it would be omitted, and the average will be performed only with the three remaining sensors. The mean obtained from the inlet sensors is then related to the TAT measurement. An alert will be triggered if the TAT increases its temperature by 2°C above the level obtained in the inlet sensors.

As can be seen in Figure 4, when the TAT tends to 0°C, an area is formed between T12 / T20 and TAT. This area is monitored by the function AREA_OVER_LIMIT shown in Figure 5. This function, by means of an upper limit (TAT) and a lower limit (T12 / T20 + 2°C), gives us:

- the time at which the event starts (t0),
- the time the event ends (tol - Ends),
- the time in which the upper limit reaches its absolute maximum (t_max),
- the area between the limits (tat_area), and
- the value of the upper limit itself.

Figure 5. AREA_OVER_LIMIT function

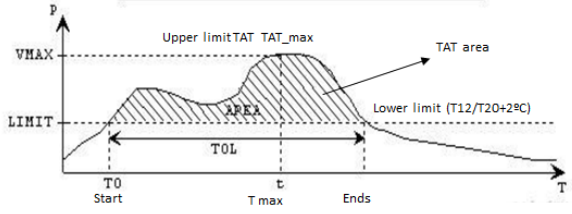

This information is used to classify TAT events in 2 categories.

Class 1 is the most unfavorable event, and will be notified if:

- The difference between TAT and the temperature at the engine inlet is higher than 2ºC (TAT-AVG (T12 / T20) > 2);
- The area AREA_OVER_LIMIT is greater than 100 (TAT_area > 100), and
- The maximum value of TAT is greater than -3°C (TAT_max > -3°C).

Class 2 is the least unfavorable event, but still noticeable. It will be notified if:

- TAT increases by 2°C above the T12 / T20 (TAT-AVG (T12 / T20) > 2);
- The area AREA_OVER_LIMIT is greater than 100 (TAT_area > 100), and
- The maximum value of TAT is greater than -10ºC and less than -3ºC (-10ºC < TAT_max < -3ºC).

This classification is designed to consider variations of TAT in a period of less than 5 min as the same event, and TAT variations separated by more than 5 minutes as differentiated events.

The flowchart in Figure 6 summarizes the improved heuristic ("TAT event": 2°C differences between the TAT and the engine's inlet temperature sensors -T12/T20-).

Figure 6. Flowchart for the improved TAT event heuristic

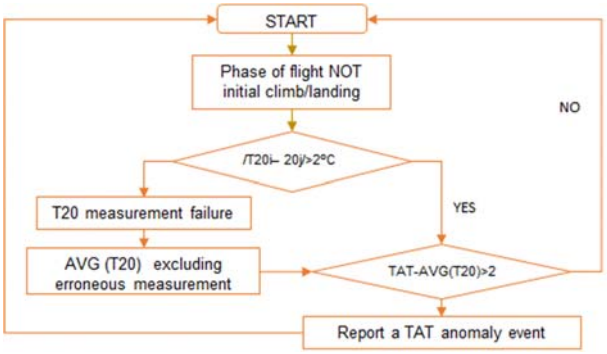

5 Exploratory analysis of TAT anomalies

The exploratory analysis of TAT anomalies covers a period of almost 4 years, from January 2012 to September 2015, and more than 285,000 flights. It includes data from different airlines, short and medium-haul fleets & long-haul fleets and worldwide routes. Table 1 shows the total flights registered during that period for the different fleets considered in the analysis. Figure 7 and Figure 8 illustrate the distribution of flights per month and fleet.

An analysis of FDM data was performed for each of these flights, to identify and detect anomalies in TAT. This analysis provides insight on the potential frequency of occurrence, location, and magnitude of HAIC.

Table 1. Flights analyzed per fleet between January 2012 and September 2015

ALL FLIGHTS	JAN	FEB	MAR	APR	MAY	JUN	JUL	AUG	SEP	OCT	NOV	DEC	TOTAL
A319-111	6247	5298	6133	6221	7139	7081	7409	6707	6637	5270	4561	3982	72685
A320-214	5695	4950	6204	5974	5786	6117	5865	5208	5599	5047	3675	3448	63568
A320-216	1042	1111	1254	1328	1582	1412	1399	1529	1718	1196	1094	1004	15669
A321-211	4940	4318	5521	5860	6212	6061	6213	6076	6317	4485	3571	3536	63110
A321-212	964	1060	1224	1168	1271	1368	1466	1335	1307	1048	825	816	13852
A330-302	632	625	785	804	1029	985	1089	1083	1007	644	626	613	9922
A340	1427	1277	1528	1492	1489	1505	1502	1549	1471	1115	1031	1050	16436
A340-642	2658	2352	2662	2540	2700	2814	3161	3056	2810	2029	1846	1870	30498
TOTAL	23605	20991	25311	25387	27208	27343	28104	26543	26866	20834	17229	16319	285740

Figure 7. Flights per month

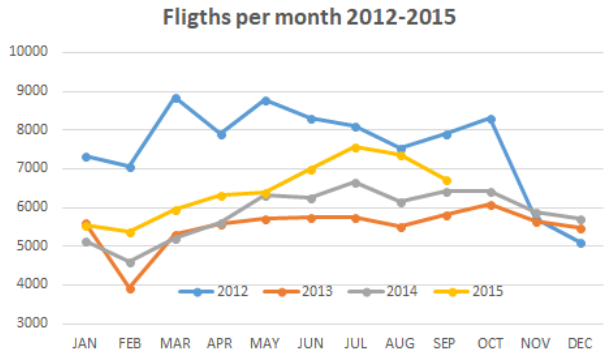

Figure 8. Flights per fleet

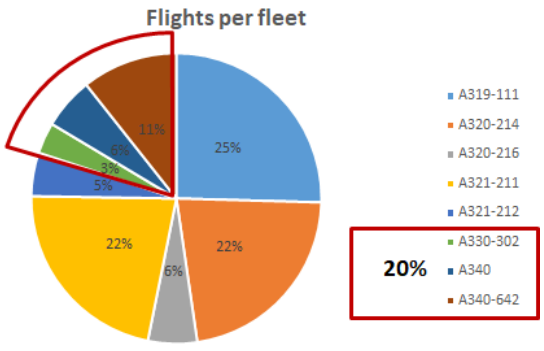

Table 2 shows the TAT events registered in each month for the different analyzed years. The rates of TAT events by number of operations reached similar values for all years, around 0,2%. A seasonal analysis shows that May, June and July are the months with the least percentage of TAT anomalies per flight. Whereas the period

between October and December presents the higher values in TAT anomalies per flight. Note that although 2015 presents a lower events/flight rate, this year does not include data from October to December, which is the peak period for TAT anomalies.

Table 2. TAT events per flight

	2012	2013	2014	2015	EVENTS/ MONTH	RATES/ MONTH
JAN	12	12	13	8	45	0,19%
FEB	14	7	13	12	46	0,22%
MAR	13	13	9	9	44	0,17%
APR	14	12	15	10	51	0,20%
MAY	14	12	4	8	38	0,14%
JUN	12	9	11	8	40	0,15%
JUL	11	4	7	11	33	0,12%
AUG	17	16	11	13	57	0,21%
OCT	26	16	22		64	0,31%
NOV	19	12	15		46	0,27%
DIC	17	14	9		40	0,25%
EVENTS/YEAR	186	140	143	92	561	0,20%
RATES/ YEAR	0,20%	0,21%	0,20%	0,16%	0,20%	

According to Figure 9 and Figure 10, short and medium-haul fleets show a smaller number of TAT events than long-haul fleets. 3/4 of TAT anomalies occurred on long haul flights (50% A340-600 - 25% A340). For short and medium-haul fleets, a higher concentration of TAT events is observed in the months from May to October. With respect to long-haul flights, the 340-600 fleet presents an increase in TAT anomalies from October to April; while for the 340 fleet there is an almost constant number of TAT events from March to April and a peak from September to November.

Figure 11 shows that TAT anomalies occurred predominantly between 16:00 and 24:00 (the period with a higher operational activity), Figure 12 shows that 90% of the TAT events occurred above 30,000 ft.

Figure 9. TAT anomalies for medium and short-range fleets

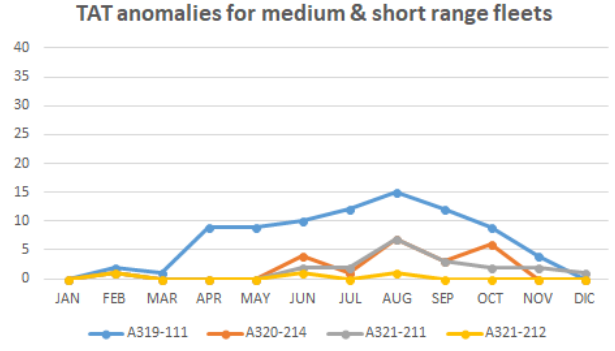

Figure 10. TAT anomalies for long haul fleets

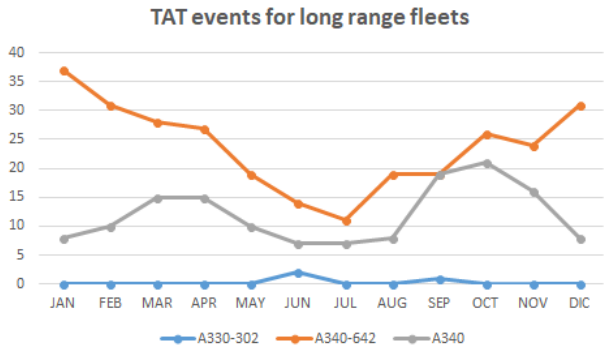

Figure 11. TAT anomalies per time of day

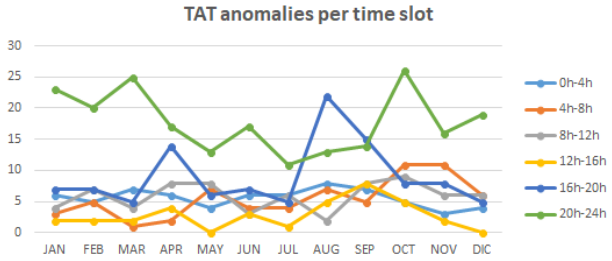

Figure 12. TAT events per flight level (FL)

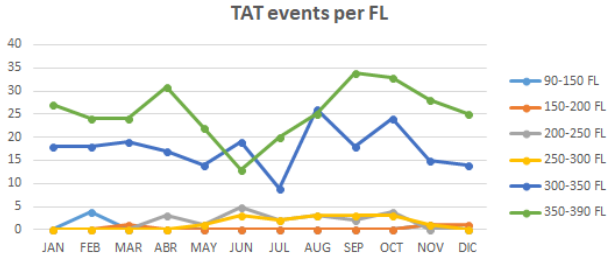

For the geographic analysis of the TAT anomalies, 6 different geographic zones are established. They are indicated in Figure 13: Center-North America, North Atlantic, Europe, South America, South Atlantic, and Africa.

Figure 14 shows that South America is the geographic area with more TAT events (287).

Figure 13. Geographic zones for TAT anomalies analysis

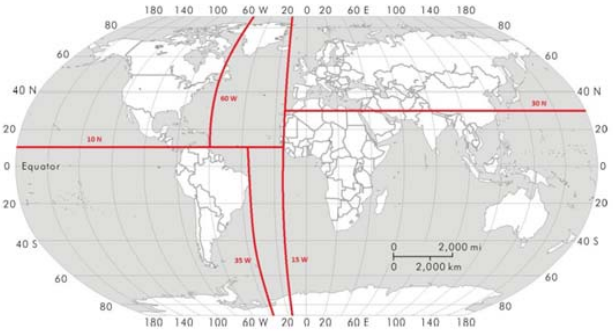

Figure 14. TAT anomalies with respect to geographical distribution

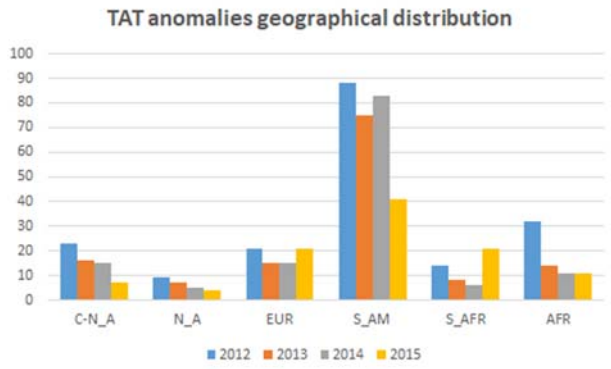

Figure 15 illustrates a more detailed analysis for the South America area. The percentage of TAT events by number of operations is almost constant (2%). The first and fourth quarters of the year display the largest number of events.

Figure 15. Geographical, monthly and fleet distribution of the TAT anomalies in the South America area

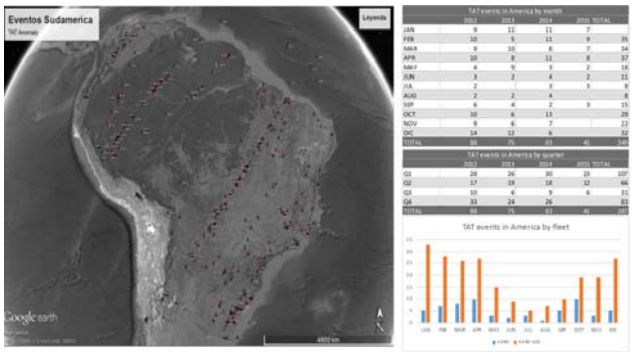

6 Route analysis

Table 3 shows the relationship between TAT anomalies and the number of operations per route. As can be seen, the route Santiago de Chile-Madrid (SCL-MAD) is the one that presents the highest number of TAT events and the highest rate of events/flight: 62 anomalies in 1,419 operations (4.3%). Figure 16 illustrates the location of TAT anomalies in the South American routes.

To draw clearer conclusions, the probability of experiencing a TAT anomaly has been calculated for each route based on a Binomial distribution, that considers the number of TAT anomalies found and the volume of operations at each route. Therefore, we performed a probabilistic analysis per route, modelling TAT events with a Binomial distribution *B (n; p)*.

Table 3. TAT anomalies per route

Route	TAT events	Flights	TAT events/flights	Probability of 1 or more TAT anomalies each 100 operations
SCL-MAD	62	1419	0,044	0,99
MAD-LIM	55	1460	0,038	0,98
MAD-EZE	47	2519	0,019	0,85
MAD-SCL	42	1390	0,030	0,95
EZE-MAD	33	2533	0,013	0,73
SSG-MAD	27	1118	0,024	0,91
LIM-MAD	20	1471	0,014	0,75
GRU-MAD	19	1935	0,010	0,63
MAD-MVD	16	489	0,033	0,96
MAD-GRU	15	1921	0,008	0,54
MAD-SSG	15	1104	0,014	0,75
MAD-UIO	12	1184	0,010	0,64
MAD-SJO	11	1241	0,009	0,59
BOG-MAD	10	1441	0,007	0,50
LOS-MAD	9	679	0,013	0,74
GIG-MAD	9	1090	0,008	0,56
MAD-BOG	9	1417	0,006	0,47
TOTAL	411	24411		

Figure 16. TAT anomalies per route (South America)

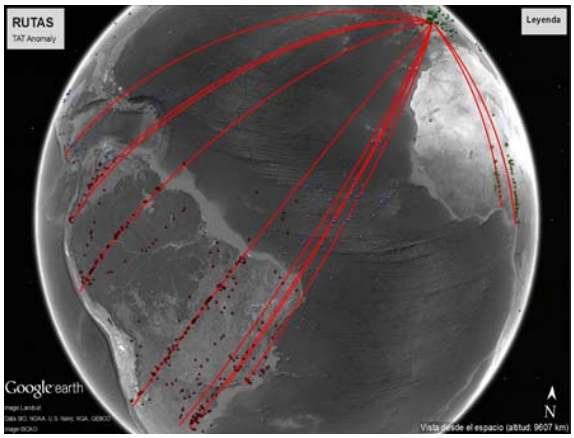

The Binomial distribution is associated to Bernoulli processes, and has the following properties:

- The experiment consists of *n* repeated attempts.
- The results of each of the attempts can be classified as either a success or a failure.
- The probability of success represented by *p* remains constant for all attempts.
- Repeated attempts are independent.

If we perform n times an experiment in which we can obtain a success, *E*, with

probability *p*, or a failure, *F*, with probability *q* (*q=1-p*), we can say the experiment follows a binomial distribution with parameters *n* and *p*, and we will represent it by *B (n; p)*. In this case, the probability of obtaining *r* successes is given by:

$$p\,(x = r) = \binom{n}{r}\, p^r\, q^{n-r} \qquad (1)$$

Where *p(x=r)* is the probability of having *r* successes in *n* experiments; consequently *(n-r)* failures. $\binom{n}{r}$ represents the number of ways of choosing *r* objects from n experiments.

With Equation (1) and the registered TAT data, we can obtain the probability of having at least 1 TAT event each 100 operations (see Table 3); we have a fixed number of trials and two types of outcomes: TAT event & NO TAT event.

- Probability of (0 TAT events) = *p (x=0)*
- Probability of (1 or more TAT events) = *1- p (x=0)*

Figure 17 and Figure 18 illustrate the analysis for the appraised routes.

Figure 17. TAT anomalies (left axis) and flights (right axis) per route

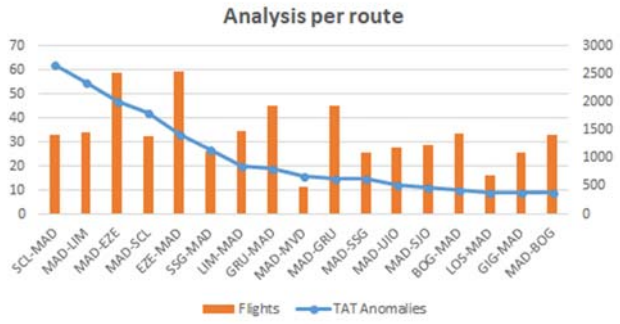

Figure 18. Probability of having more than 1 TAT event each 100 operations per route (left axis) and total TAT anomalies (right axis)

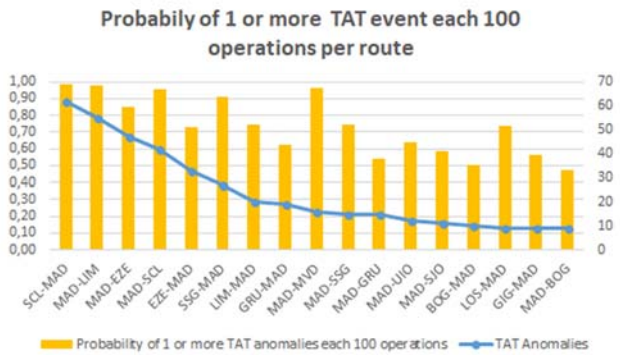

Table 4 shows the monthly risk analysis of the most unfavourable routes (probability of having at least 1 TAT event each 100 operations). Certain routes present TAT events on both outbound and return flights, making them particularly relevant for the study.

Table 4. Probability of having at least 1 TAT event each 100 operations

MAD-SCL-MAD	MAD-EZE-MAD	MAD-LIM-MAD	MAD-SGS-MAD	MAD-GRU-MAD	MAD-MVD-MAD	MAD-BOG-MAD
JAN	JAN	JAN	JAN	JAN	JAN	JAN
FEB	FEB	FEB	FEB	FEB	FEB	FEB
MAR	MAR	MAR	MAR	MAR	MAR	MAR
APR	APR	APR	APR	APR	APR	APR
MAY	MAY	MAY	MAY	MAY	MAY	MAY
JUN	JUN	JUN	JUN	JUN	JUN	JUN
JUL	JUL	JUL	JUL	JUL	JUL	JUL
AUG	AUG	AUG	AUG	AUG	AUG	AUG
SEP	SEP	SEP	SEP	SEP	SEP	SEP
OCT	OCT	OCT	OCT	OCT	OCT	OCT
NOV	NOV	NOV	NOV	NOV	NOV	NOV
DIC	DIC	DIC	DIC	DIC	DIC	DIC
SOUTH AMERICA	SOUTH AMERICA	SOUTH AMERICA	AFRICA	SOUTH AMERICA	SOUTH AMERICA	SOUTH AMERICA

	High Probabiltiy of a TAT event	80% < TAT event <100%
	Medium probability of a TAT event	50% < TAT event probability <80%
	Low probability of a TAT event	0% < TAT event <50%
	NO probability of a TAT event	0% TAT event

The route Madrid-Santiago de Chile-Madrid (MAD-SCL-MAD) is the one with the highest number of quantified TAT events: a total of 104 events, between January 2012 and September 2015, in 2,809 operations (3.7%). This route usually has an average of 61 operations per month, with a minimum of 51 operations and a maximum of 88 operations. According to the calculations, the probability of a TAT anomaly occurring every 100 flights is 97.70%. Figure 19 illustrates the monthly probability of having at least 1 TAT event each 100 operations for the Madrid-Santiago de Chile-Madrid route.

Figure 19. Probability of having at least 1 TAT event each 100 operations for the MAD-SCL-MAD route (left axis) and TAT events (right axis)

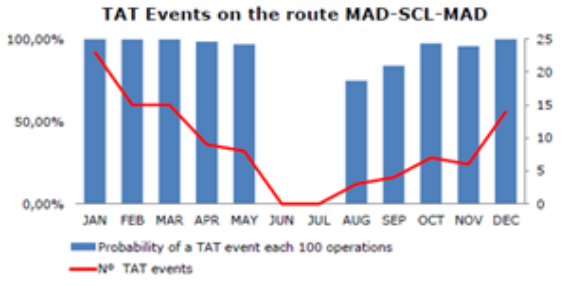

The probabilities of a TAT event occurring every 100 flights for other routes are: 92.51% (Madrid-Lima-Madrid), 85.91% (Madrid-Montevideo-Madrid), 85.17% (Madrid-Malabo-Madrid), 79.73% (Madrid-Buenos Aires-

Madrid), 59.82% (Madrid-São Paulo-Madrid) and 48.68%. (Madrid – Bogotá-Madrid).

7. Conclusions and future work

High Altitude Concentrations of Ice Crystals (HAIC) constitute a hazard to air transport operations. They can cause engine power loss, as well as engine compressor damage due to ice shedding. Along with these events, disruption to aircraft systems are noted when HAIC are ingested into air data probes, causing erroneous measurements of temperature and air speed. Airplane Total Air Temperature (TAT) probe erroneously reporting 0°C, or in error, is known to be evidence of ice crystals in the atmosphere. TAT events have been analysed from FDM (Flight Data Monitoring) data for two families of engines and more than 285,000 flights. A detection heuristic, which is tolerant to sensor failure, has been developed. It generates a reliable indicator, based on the differences between the TAT and the engine's inlet temperature sensors, to provide early warning to pilots of high concentrations of ice crystals. Exploratory analysis of the TAT events provides insight on the frequency of occurrence, location, and magnitude of these anomalies and potential HAIC conditions. TAT events peak at October, long-haul flights, time-period between 16:00 and 24:00, altitude above 30,000 ft and South America. The probability of experiencing 1 or more TAT events per route has been calculated as a risk of HAIC indicator for the most affected routes. Further work might be focused on: (i) increasing insight on the frequency of occurrence, location, and magnitude of HAIC events; (ii) improving real time HAIC detection and awareness: e.g., Aircraft Communications Addressing and Reporting System (ACARS) alert triggered by TAT events; (iii) boosting cooperative programs between companies for FDM exploitation in an overall TAT monitoring project: (iv) coordinating the TAT events analysis with maintenance programs; (v) developing a possible use of TAT events as a HAIC risk indicator; and (vi) exploring how worldwide TAT anomalies data can be used to improve meteorological predictive models and HAIC maps.

References

[1] F. Dezitter, A. Grandin, J.L. Brenguier, F. Hervy, H. Schlager, P. Villedieu, G. Zalamansky, HAIC (High Altitude Ice Crystals), 5th AIAA Atmos. Sp. Environ. Conf. Aircr. Icing. (2013). doi:10.2514/6.2013-2674.

[2] J.A. Haggerty, J.B. Jensen, K.E. Schick, C. Yost, High Ice Water Content and Airborne Temperature Measurement Anomalies in Tropical Convection, in: 96th Am. Meteorol. Soc. Annu. Meet., New Orleans, LA, 2016.

[3] M.L. Grzych, J.G. Mason, Weather Conditions Associated with Jet Engine Power-loss and Damage Due to Ingestion of Ice Particles: What We've Learned Through 2009, in: Am. Meteorol. Soc. 14th Conf. Aviat. Range, Aerosp. Meteorol., 2010.

[4] BEA, Final report on the accident on 1st June 2009 to the Airbus A330-203 registered F-GZCP operated by Air France flight AF 447 Rio de Janeiro - Paris, Le Bourget Cedex - France, 2009. https://www.bea.aero/docspa/2009/f-cp090601.en/pdf/f-cp090601.en.pdf.

[5] N. Cisse, Accident on 24 July 2014 in the region of Gossi in Mali to the MD-83 registered EC-TV operated by Swiftair S.A, 2014. https://www.bea.aero/docspa/2014/ec-v140724.e1.en/pdf/ec-v140724.e1.en.pdf.

[6] A. Hamed, K. Das, D. Basu, J.G. Mason, Current perspectives on jet engine power loss in ice crystal conditions: Engine icing, 5th AIAA Atmos. Sp. Environ. Conf. (2011). doi:10.1115/1.4002020.

[7] J.G. Mason, P. Chow, D.M. Fuleki, Understanding Ice Crystal Accretion and Shedding Phenomenon in Jet Engines Using a Rig Test, J. Eng. Gas Turbines Power. (2011). doi:10.1115/1.4002020.

[8] C. Schewie, M.R. Daup, J.W. Nelson, Aircraft Toatal Air Temperature Anomaly Detection, US 2016/0370236 A1, 2016.

[9] D. Leroy, E. Fontaine, A. Schwarzenboeck, J.W. Strapp, Ice Crystal Sizes in High Ice Water Content Clouds, J. Atmos. Ocean. Technol. 34 (2017) 117–136. doi:10.1175/JTECH-D-15-0246.1.

[10] A.B. Flegel, Ice Crystal Icing Research at NASA, 9th AIAA Atmos. Sp. Environ. Conf. (2017). doi:10.2514/6.2017-4085.

[11] J.C. Tsao, P. Struk, M. Oliver, Possible mechanisms for turbofan engine ice crystal icing at high altitude, in: 6th AIAA Atmos. Sp. Environ. Conf., Atlanta, GA, 2014. doi:10.2514/6.2014-3044.

[12] M. De Reus, S. Borrmann, A. Bansemer, A.J. Heymsfield, Evidence for ice particles in the tropical stratosphere from in-situ measurements, Atmos. Chem. Phys. (2009). doi:10.5194/acp-9-6775-2009.

Copyright Statement